

# LOW TEMPERATURE THERMAL BEHAVIOUR OF ELECTRODEPOSITED NANOCRYSTALLINE NICKEL COATINGS ON MILD STEEL SUBSTRATE

Haitao Ni, Jiang Zhu, Zhaodong Wang and Haiyang Lv

College of Materials and Chemical Engineering, Chongqing University of Arts and Sciences, Yongchuan, Chongqing 402160, China

Received: May 15, 2017

**Abstract.** The nanocrystalline nickel coating with a relatively narrow size distribution ranging from 20 nm to 60 nm was produced by electrodeposition on the mild steel substrate. Effects of annealing time on microstructure and microhardness evolution of the as-deposited nanocrystalline nickel coating at 150 °C were investigated. The results showed that a four-hour low temperature annealing has no obvious effect on the (200) preferred orientation of the as-deposited coating. Further quantitative X-ray analysis based on line broadening revealed grain growth occurs in spite of annealing the sample at a relative low temperature. The Vickers microhardness indicated that the as-deposited nanocrystalline nickel coating exhibits a combination of annealing hardening followed by annealing softening with increasing annealing time. It was suggested the annealing hardening was mainly due to grain boundary relaxation for the sample annealed within 60 min, while the annealing softening was mainly due to grain coarsening for the sample annealed beyond 60 min.

## 1. INTRODUCTION

In the modern manufacturing and processing industries, many parts or components put forward higher demands for the materials with comprehensive performances such as high strength, corrosion resistance and abrasion resistance. However, it is difficult to satisfy multiple requirements based solely on material selection or structure design. Meanwhile, such requirements should pay high costs. In view of the fact several machine parts or components are made of steel, the coating technology has extensively been used as an effective and economic way to protect the metal surface from corrosion and abrasion [1-6]. Previous investigations have demonstrated that the nickel coating produced by electroplating/electrodepositing can effectively improve the corrosion resistance and wear resistance of steel substrate [5-8]. Especially to deserve to be men-

tioned, some researchers have made efforts to explore enhanced performance optimization of nickel coating electroplated on Q235A mild steel [8].

Until now, more and more facts have shown that the traditional coating materials with a micron size have almost reached the feasible limit of achievable performance, while the nanocrystalline (NC) materials with a grain size of typically less than 100 nm can further provide some excellent performance [9-13]. Due to a significant increase in hardness, wear resistance and local corrosion resistance, NC nickel and its alloys are expected to become protective coating materials with more superior performance. On the other hand, sometimes in the actual service process, thermal effect on microstructure and property of NC materials should be considered. Most studies suggest that the tiny grains have strong tendency to grow upon heating and grain growth is very sensitive to temperature [14-17]. In particularly, the

---

Corresponding author: Haiyang Lv, e-mail: lvhaiyang89@163.com

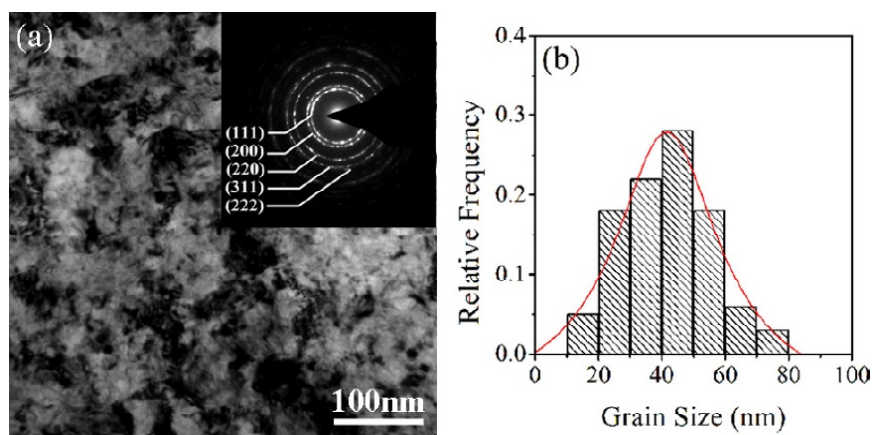


**Fig. 1.** Typical bright-field TEM images and statistical grain size distributions for the as-received NC nickel coating.

influence of low temperature annealing on grain growth of electrodeposited NC nickel with an average grain size of 29 nm has been investigated [14]. The results indicated that there was little change in the grain size after annealing for 1 h at temperatures below 150 °C. However, some grains grew up and a bimodal grain size distribution was obtained when the annealing was done at 200 °C, while the grain size would reach micron level with further annealing at above 250 °C. Thermal stability of electrodeposited NC Ni-Co-Fe alloy coatings shown that the grain grew slowly during annealing below 375 °C, while the rapid grain growth concurrent with a strong (111) texture occurred during annealing above 450 °C [18].

In light of this, considering that it is sometimes inevitable to use machine parts or component containing NC counterparts at elevated temperature, the present study therefore focused on the effect of low temperature annealing on electrodeposited NC nickel coating on mild steel substrate, expecting to provide theoretical guidance for the application of NC coating under a higher temperature.

## 2. EXPERIMENTAL

In the present investigation, mild steel was used as the substrate for plating. Mild steel sheets of size 20 mm length and 12 mm width were successively treated by degrease, alkali cleaning, acid cleaning and chemical activation before plating. A modified Watts-type bath was chosen for electrodepositing NC nickel coating onto a well-polished mild steel substrate. The plating bath composition and conditions used were similar to those used by Dai et al. with slight modifications [19]. The plating was done to get a coating thickness of about 100  $\mu\text{m}$ .

The as-deposited samples were annealed in vacuum at 150 °C for various times of 30 min to 240 min. Differential scanning calorimetry (DSC) analyses was used to evaluate overall thermal behaviour of the electrodeposited nanocrystalline coatings. DSC studies was performed on NETZSCH STA449C at 20 °C  $\text{min}^{-1}$  heating rate and purged by pure Ar (99.999% purity) at 80  $\text{ml}\cdot\text{min}^{-1}$ . The as-deposited sample was first heated to 400 °C. After cooling, the sample was reheated to 400 °C for the purpose of reference only.

The microstructures of the as-deposited and annealed samples were investigated by X-ray diffraction (XRD) and transmission electron microscopy (TEM). XRD measurements were performed on a Rigaku D/MAX RC diffractometer operating in a step scan mode with Cu  $K\alpha$  radiation, using an accelerating voltage of 40 kV and a current of 150 mA, respectively. Samples for TEM observation were prepared by double-jet electropolishing at 20 V (DC) using a solution of nitric acid and methanol (V:V=1:4) at -30 °C. Grain size distribution was observed under a Zeiss Libra 200FE TEM operated at 200 kV.

Microhardness measurements were carried out by a Vickers hardness indenter using a load of 0.98 N for a dwell time of 15 s during testing. An average of 10 readings was taken to obtain the microhardness values of the NC nickel coatings.

## 3. RESULTS AND DISCUSSION

Fig. 1 shows the TEM results on the microstructure of as-received NC nickel coating electrodeposited on mild steel. No cracks or hollows could be found from TEM observation. The bright-field TEM image reveals that the grain shapes are equiaxed. The

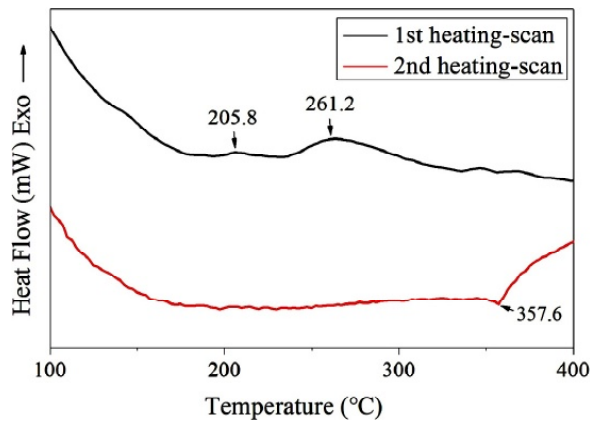


Fig. 2. Typical DSC curve of NC nickel coating.

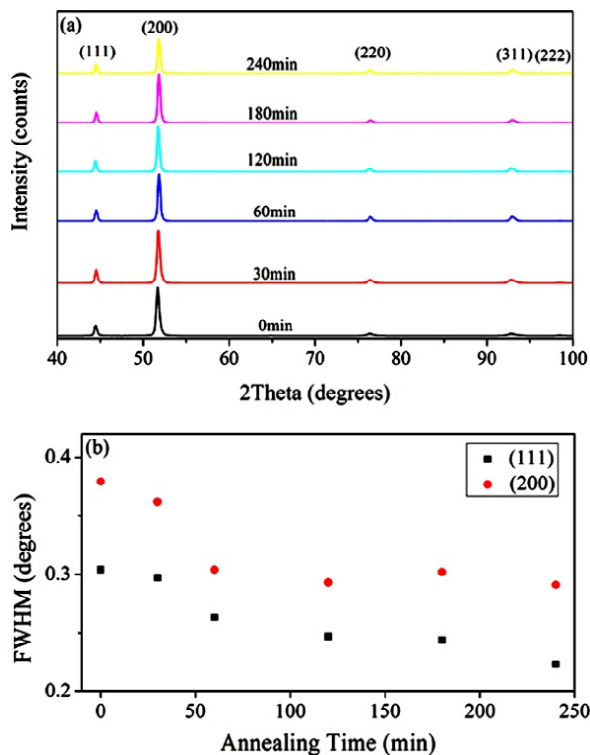


Fig. 3. XRD patterns for annealed NC nickel coating with various times and corresponding FWHM of (111) and (200) reflections.

existence of the face-centered-cubic (FCC) structure can be observed from the diffraction pattern as shown in the inset of Fig. 1a. The corresponding grain-size distribution is also given in Fig. 1b, indicating a relatively narrow distribution of grain sizes. More than 80% of grains range in size from 20 nm to 60 nm. Based on counting results of 200 grains, the average grain size of as-received NC nickel coating is calculated to be about ~43 nm.

Fig. 2 presents the DSC curves of the as-received NC nickel coating. During the first DSC heating scan, exothermic peaks at 205.8 °C and 261.2 °C are believed to be due to grain growth and well demon-

strated as a result of grain boundary activities [15,16]. Especially the exothermic peak at 261.2 °C, quantitative analysis shows that the grain growth process involves an energy release of 4.04 J/g, causing an exothermic peak with an onset temperature of ~230 °C. However, only Curie transformation point at 357.6 °C is observed during the second DSC heating scan. Since the determined Curie temperature agrees well with the data for the coarse-grained nickel, it can be concluded the nanograins in as-deposited NC nickel have grown into micrograins before the second heating-scan [20-21].

Fig. 3 shows XRD patterns of the NC coating with various annealing times at 150 °C. It is obvious that in the as-deposited NC nickel coating only a FCC phase was identified. By comparing the XRD pattern of standard nickel sample with a complete random orientation (PDF#04-0850), it can be seen from Fig. 3a that the as-deposited coating exhibits a significant preferred (200) orientation. When annealing is conducted, various annealing times has no obvious effect on the (200) preferred orientation. Note that the temperature dependence of grain growth is well recognized, attention is focused on X-ray line profile analysis. As shown in Fig. 3b, quantitative analyses of the full width at half maximum (FWHM) of (111) and (200) reflections indicate that there is an obvious decrease in FWHM, which may be due to grain growth and/or strain release [15,22-23]. Previous studies have suggested that the grain growth process in electrodeposited NC Cu samples an average grain size of 30 nm occurs prior to the microstrain release process [22].

Fig. 4 shows the grain size of samples determined by XRD analysis. The average grain size of the as-deposited sample is ~39 nm, which is smaller than that determined by TEM. This discrepancy can

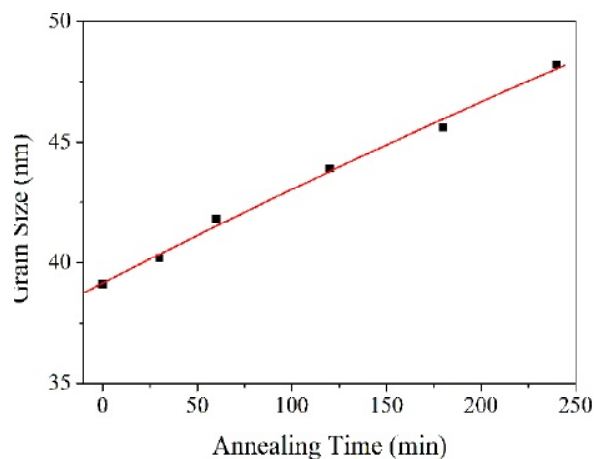
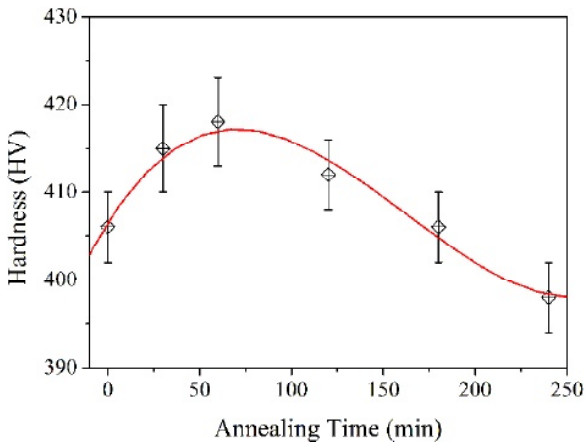
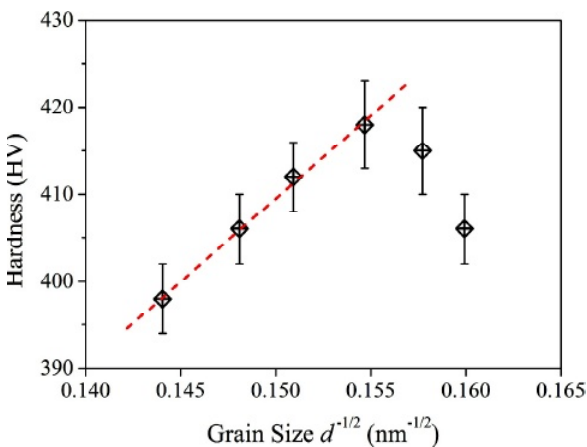


Fig. 4. Grain size of NC nickel coating as a function of annealing time.



**Fig. 5.** Change of Vickers hardness (HV) for as-deposited NC nickel coating as a function of annealing time.



**Fig. 6.** Vickers hardness (HV) of NC nickel coating as a function of the grain size in terms of Hall-Petch relationship.

be attributed to different structure characterization approaches [24]. After annealing at 150 °C for 30 min, the grain size increases to ~40 nm. With increasing annealing time, the grain size continues to increase. The grain size of the sample annealed for 240 min reaches ~48 nm. Such a continuous increase in grain size indicates that grain growth occurs during long-term annealing process despite at a relative low temperature.

Fig. 5 shows the hardness evolution of NC nickel coating during isothermal annealing process for different annealing times at 150 °C. The hardness of the as-deposited sample is ~406 HV. When the as-deposited sample is annealed, it is found that the hardness starts to increase and reaches a peak value ~418 HV for 60 min. However, with increasing annealing time, the hardness subsequently goes downwards. The hardness of the samples annealed for 240 min drops to ~398 HV, which is even lower

than the hardness of the as-deposited state. To better understand the correlation between microhardness and microstructure of NC nickel coating, the evolution of Vickers hardness as a function of the grain size in terms of Hall-Petch relationship is redrawn in Fig. 6. It can be found the hardness is in agreement with the inverse square-root of the grain size ( $d^{1/2}$ ) when the annealing time exceeds 60 min at 150 °C.

On the basis of the above microstructure and performance analysis, the combination of hardening followed by softening can be explained by unique nanostructure in NC samples. Recently some experiments have shown annealing hardening phenomenon in NC metals and alloys [14,25-27]. It has been reported that internal stresses may be restored partially by grain boundary atom readjustments in low temperature annealing. Such grain boundary relaxation will lead to an increased difficulty for grain boundary emission of dislocations. Due to an increase in the stress required to activate new dislocation sources, the annealed sample exhibits hardening during the microhardness measurements. On the other hand, with increasing annealing time of up to 240 min, an obvious coarsening of the nanograins occurs, the mechanism for the emission of partial dislocations from grain boundaries no longer plays a major role. Similar to conventional coarse-grained nickel, the microhardness of the NC nickel coating will drop down with increasing grain size on the basis of the Hall-Petch relationship [28].

#### 4. CONCLUSION

In this work, the nanocrystalline nickel coating was electrodeposited on a mild steel substrate. Transmission electron microscopy observations revealed that the as-deposited coating has a narrow grain size distribution ranging from 20 nm to 60 nm. Differential scanning calorimetry suggested that the as-deposited nanocrystalline coating has an obvious grain growth trend at annealing temperature above 200 °C. The as-deposited samples were then annealed in vacuum at 150 °C from 30 min to 240 min. X-ray diffraction patterns showed that long-term annealing has no obvious effect on the (200) preferred orientation of the as-deposited coating. Despite of annealing at a relative low temperature, a general increasing grain size trend with increasing annealing time was still observed from X-ray diffraction analysis based on line broadening. The Vickers microhardness indicated that the as-deposited coating exhibits a combination of hardening followed by softening. It was suggested the increase in

microhardness was due to grain boundary relaxation for the sample annealed within 60 min, while the decrease in microhardness was due to grain coarsening for the sample annealed beyond 60 min.

## ACKNOWLEDGEMENTS

This work was supported by the National Natural Science Foundation of China (№ 51601026) and the Science and Technology Research Project of Chongqing Municipal Education Commission of China (KJ1601134).

## REFERENCES

- [1] E. Lugscheider and T. Weber // *Fresenius J. Anal. Chem.* **333** (1988) 293.
- [2] S.L. Lee, D. Windover, M. Audino, D.W. Matson and E.D. McClanahan // *Surf. Coat. Technol.* **149** (2002) 62.
- [3] D. Rajput, K. Lansford, L. Costa and W. Hofmeister // *Surf. Coat. Technol.* **203** (2009) 1281.
- [4] M.E. Sahayaraj, J.T.W. Jappes, I. Siva and N. Rajini // *Science and Engineering of Composite Materials* **23** (2016) 309.
- [5] C.N. Panagopoulos and V.D. Papachristos // *J. Mater. Sci.* **31** (1996) 2931.
- [6] T. Tüken, B. Yazýc and M. Erbil // *Mater. Des.* **28** (2007) 208.
- [7] F. Sun, G. Meng, T. Zhang, Y. Shao and F. Wang // *Electrochim. Acta* **54** (2009) 1578.
- [8] M. Liu, Y. Meng, Z. Yang, F. Li, Y. Gong and L. Feng // *Surf. Coat. Technol.* **286** (2015) 285.
- [9] K. Wei, Y. Fu, X. Wu, S.Z. Yang and B. Li // *J. Mater. Eng. Perform.* **8** (1999) 521.
- [10] Q. Li, H. Lu, J. Cui, M. An and D. Li // *Surf. Coat. Technol.* **304** (2016) 567.
- [11] B.A. Bouwhuis, T. Ronis, J.L. Mccrea, G. Palumbo and G.D. Hibbard // *Compos. Sci. Technol.* **69** (2009) 385.
- [12] G. Gupta, K. Mondal and R. Balasubramaniam // *J. Alloys Compd.* **482** (2009) 118.
- [13] C. Gu, J. Lian, J. He, Z. Jiang and Q. Jiang // *Surf. Coat. Technol.* **200** (2006) 5413.
- [14] Y.M. Wang, S. Cheng, Q.M. Wei, E. Ma, T.G. Nieh and A. Hamza // *Scripta Mater.* **51** (2004) 1023.
- [15] L. Lu, L.B. Wang, B.Z. Ding and K. Lu // *Mater. Sci. Eng. A* **286** (2000) 125.
- [16] M. Thuvander, M. Abraham, A. Cerezo and G.D.W. Smith // *Mater. Sci. Technol.* **18** (2001) 151.
- [17] U. Klement and M.D. Silva // *J. Iron Steel Res. Int.* **14** (2007) 173.
- [18] L.B. Lin, L.F. Lin, P.Q. Dai, Y.X. Liao and Y.B. Zheng // *Chin. J. Nonferrous Met.* **21** (2011) 1087.
- [19] P. Q. Dai, H. Yu and Q. Li // *Transactions of Materials and Heat Treatment* **25** (2004) 1283.
- [20] R.Z. Valiev, G.F. Korznikova, Kh.Ya. Mulyukov, R.S. Mishra and A.K. Mukherjee // *Philos. Mag. B* **75** (1997) 803.
- [21] B. Legendre and M. Sghaier // *J. Therm. Anal. Calorim.* **105** (2011) 141.
- [22] L. Lu, N.R. Tao, L.B. Wang and B.Z. Ding // *J. Appl. Phys.* **89** (2001) 6408.
- [23] A. Kumpmann, B. Günther and H.D. Kunze // *Mater. Sci. Eng. A* **168** (1993) 165.
- [24] Y. Zhong, D. Ping, X. Song and F. Yin // *J. Alloys Compd.* **476** (2009) 113.
- [25] X.Y. Zhang, Q. Liu, X.L. Wu and A.W. Zhu // *Appl. Phys. Lett.* **93** (2008) 261907.
- [26] T.J. Rupert, J.R. Trelewicz and C.A. Schuh // *J. Mater. Res.* **27** (2012) 1285.
- [27] Z.H. Cao, P.Y. Li, L. Wang, Z.H. Jiang and X.K. Meng // *Appl. Phys. A* **109** (2012) 613.
- [28] E.O. Hall // *Nature* **173** (1954) 948.